International Journal of Scientific Research in Engineering and Management (IJSREM)
Volume: 09 Issue: 11 | Nov - 2025 SJIF Rating: 8.586 ISSN: 2582-3930

Comparative Structural Performance Analysis of Castellated and Rolled Steel Beams in Pre-Engineered Building Systems

Akshay Bhattad, Prof. Shrikant M Kale

[1]Student, N. K. Orchid College of Engineering & Technology, Solapur, Maharashtra 413002

[2]Assistant Professor, N. K. Orchid College of Engineering & Technology, Solapur, Maharashtra 413002

Corresponding Author: akshaybhattad20@gmail.com

ABSTRACT

This study investigates the structural performance of castellated beams integrated into Pre-Engineered Building (PEB) systems and compares them with conventional rolled steel beams using finite element analysis (FEA). Castellated beams, created by introducing web openings in rolled I-sections, enhance load-carrying capacity, stiffness, and material efficiency, making them particularly suitable for long-span applications. The research analyzes parameters such as total deformation, normal stress, shear stress, and strain distribution under different loading conditions, adhering to IS 800:2007 and IS 875 design provisions. Results reveal that castellated beams significantly reduce stresses and deformations compared to tapered sections, demonstrating improved strength-to-weight ratios and cost efficiency. However, stress concentration around openings highlights the necessity for optimized hole geometry and detailing to prevent local failure. The case study of a PEB shed in Pune validates the applicability of castellated beams in real-world conditions, emphasizing their role in minimizing foundation loads and enhancing serviceability. Overall, castellated beams emerge as a sustainable and economical solution for modern steel construction, offering superior performance when reinforced with proper design modifications. The findings contribute valuable insights for updating design codes and guiding practical applications in industrial and commercial infrastructure.

Keywords: Castellated beams, Pre-Engineered Buildings, Structural performance, Finite Element Analysis, Stress distribution, Material efficiency

I. INTRODUCTION

The development of castellated beams dates back to the 1950s, when engineers sought to enhance the load-carrying capacity of standard rolled steel sections without increasing their self-weight. By cutting the web of an I-beam in a zig-zag pattern and welding the halves with an offset, a deeper section with hexagonal or octagonal openings is obtained. This modification increases the beam depth by approximately 40–60%, thereby improving its moment of inertia and bending strength while maintaining the same mass. Over time, castellated beams have been widely adopted in industrial, commercial, and institutional structures for their structural efficiency, material economy, and ability to accommodate mechanical, electrical, and plumbing (MEP) services through web openings. Parallelly, the concept of Pre-Engineered Buildings (PEBs) emerged in the 1960s and gained prominence in India after 2000, driven by the need for rapid, cost-effective construction solutions. PEB systems, characterized by prefabricated components and bolted assembly, offer significant reductions in construction time and overall project costs compared to conventional steel buildings.

The synergy between castellated beams and PEBs lies in their common objectives of weight reduction, span optimization, and cost efficiency. Castellated beams typically offer 20–30% higher load-carrying capacity than their parent beams, enabling larger column-free spans of up to 30–40 meters. Their integration in PEB frames not only improves functional adaptability but also reduces foundation costs by minimizing structural self-weight. However, despite these advantages, castellated beams exhibit complex behaviors such as web post buckling, Vierendeel bending, and increased susceptibility to torsional effects. Recent studies using finite element tools such as ANSYS, highlight the need to optimize hole geometry and stiffening techniques to ensure safety and serviceability. In India, the rapid growth of PEB systems and increasing application of castellated beams underscore the importance of comprehensive performance studies. A comparative evaluation with conventional I-beams under various loading conditions will provide critical insights for updating design guidelines and promoting sustainable, cost-effective, and efficient steel construction.

Fig 1. Castellated Beam

1.1 Problem Statement

Pre-Engineered Building (PEB) systems are increasingly preferred in modern construction for their cost-effectiveness, rapid erection, and optimized use of materials. Among the structural elements incorporated in PEBs, castellated beams have attracted attention due to their enhanced depth-to-weight ratio, higher stiffness, and ability to span longer distances with minimal material consumption. Despite these advantages, castellated beams introduce certain complexities arising from their web openings, including stress concentration, reduced shear capacity, and susceptibility to buckling. These behaviors can significantly influence the ultimate strength, deflection characteristics, and overall serviceability of the structure. A

major challenge lies in the insufficient understanding of castellated beam performance under diverse loading conditions, particularly lateral loads, concentrated loads, and combined bending–shear effects. Interaction of openings with connection details, lateral–torsional buckling, and local buckling mechanisms remains a critical concern. Furthermore, current design codes provide limited guidance on optimization parameters such as hole diameter-to-depth ratios and spacing, often resulting in either over-conservative or unsafe designs.

This gap in knowledge restricts structural engineers from fully utilizing the benefits of castellated beams in PEB applications. Hence, a comprehensive comparative study of castellated and solid-web beams is essential to establish benchmarks, validate performance through simulations and experiments, and provide design recommendations for safe and economical implementation.

1.2 Objectives of the study

1. To compare structural behavior of castellated and solid web I-beams in PEB structures.
2. To study effects of hole diameter and spacing on castellated beam performance under loads.
3. To evaluate base shear, drift, bending moment, axial, shear force, and torsion parameters.
4. To conduct a parametric study for optimal castellated beam design balancing efficiency and economy.

II. RELATED WORK

Jamadar, A. M., & Kumbhar, P. D. (2015) Jamadar and Kumbhar's research focuses on a parametric study of castellated beams with circular and diamond-shaped openings. They use finite element analysis to investigate how different opening shapes affect the beam's load-carrying capacity and deflection. Their study finds that diamond-shaped openings provide superior structural performance compared to circular openings, making them a better choice for large-span structural applications. This work helps in understanding the relationship between web opening shapes and structural efficiency in castellated beams.

Rodrigues, F., & Silva, A. (2015) Rodrigues and Silva focus on the finite element modeling of castellated beams with web openings. Their research analyzes how different opening shapes and sizes, such as circular, square, and triangular, influence the stress distribution, bending moments, and shear forces within the beams. By conducting various load tests using FEA, they provide detailed insights into how these design modifications affect structural performance. Their findings offer valuable guidelines for optimizing beam designs in large, light-weight structures, demonstrating the potential for castellated beams to reduce material consumption without sacrificing strength or stability.

Alshimmeri, A. J. H., & Al-Mahaidi, R. (2019) This study compares the structural performance of castellated beams and rolled steel beams with various strengthening techniques. Using finite element analysis, the authors evaluate factors such as load distribution, bending, and shear forces. The results show that castellated beams can be more efficient than traditional rolled beams in terms of material usage and performance under dynamic loading conditions. This research is crucial for improving the design of structural systems where weight reduction is essential without compromising structural integrity, such as in industrial and high-rise buildings.

Hadeed, S. M., & Alshimmeri, A. J. H. (2023) Hadeed and Alshimmeri explore the replacement of traditional trusses with tapered castellated beams in Pre-Engineered Building (PEB) structures. Their research utilizes finite element analysis to demonstrate that tapered castellated beams offer superior load distribution, material efficiency, and structural performance compared to conventional trusses. The study highlights how tapered beams reduce the need for excessive material use while enhancing structural stability. These findings make tapered castellated beams a promising solution for modern industrial and commercial PEB construction projects.

Mohan, R., & Prabhakaran, P. (2016) Mohan and Prabhakaran's research investigates the deflection characteristics of steel beams with and without web openings. Using finite element analysis, they compare the behavior of solid beams to castellated beams, focusing on the impact of web openings on deflection and overall structural performance. The study concludes that the introduction of web openings can significantly reduce deflection without compromising the strength of the beams, making castellated beams a viable option for lightweight, efficient structural designs. Their work is instrumental in guiding engineers to optimize beam designs for both strength and material savings.

Patil, D. D., & Agrawal, V. A. (2016) Patil and Agrawal's study investigates the parametric effects of web openings on steel beams, focusing on factors like the size and position of the openings. Their finite element analysis demonstrates how different configurations of web openings influence the beam's bending and shear resistance. They provide guidelines for optimizing beam designs that balance the need for material savings with the structural integrity required for heavy-duty applications. This study is valuable for industries where weight reduction and cost efficiency are critical factors without compromising structural strength.

III. PROPOSED METHODOLOGY

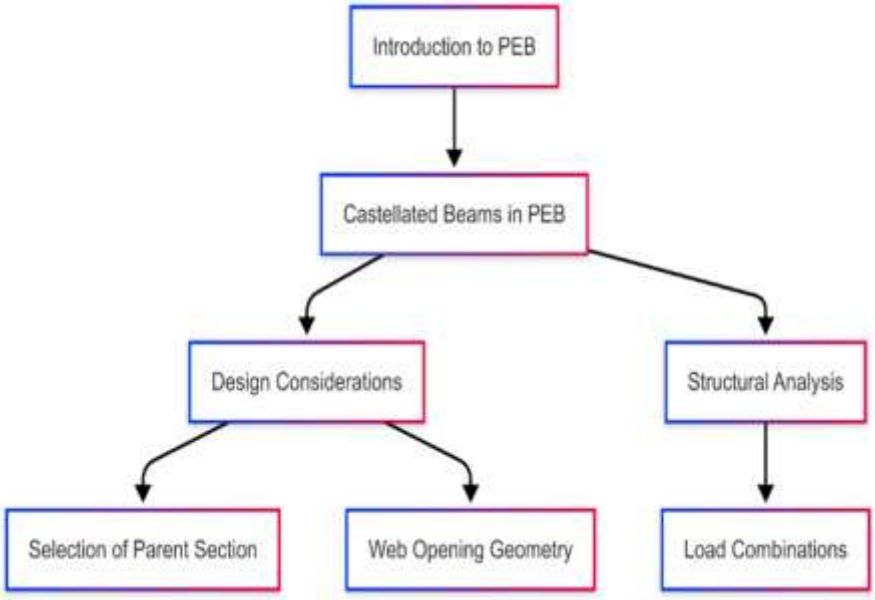

Fig 2. Proposed Methodology

The present study adopts a systematic approach to evaluate the structural performance of castellated beams in Pre-Engineered Building (PEB) systems. Standard rolled steel sections (ISMB 150, ISMB 125, and ISMB 100) as per IS 808:1989 are selected as parent beams. These sections are modified by introducing sinusoidal web openings with fillet radii of ¼, ⅛, and ⅛ of the opening depth, fabricated through oxy-cutting and rewelding in accordance with IS 816:1969 and IS 9595:1996. The resulting castellated beams are expected to achieve higher stiffness and moment capacity without additional material usage.

Structural property calculations, including moment of inertia, section modulus, and shear area, are performed for both parent and castellated beams. Safety checks for bending, shear, deflection, and lateral–torsional buckling are carried out following IS 800:2007 and IS 875 load provisions. Finite Element Analysis (FEA) is conducted in ETABS, where PEB frames incorporating both castellated and solid-web beams are modeled under dead, live, wind, and seismic loads. Load combinations are applied as per IS 875 and IS 1893:2016 to simulate realistic conditions. A parametric study further examines the influence of whole size, spacing, and beam depth on structural performance. Comparative results guide the development of design recommendations for efficient application of castellated beams in PEB structures.

3.1 ANSYS PROPERTY PAGE

1. SOLID186

SOLID186 is a higher-order 3D solid element in ANSYS with 20 nodes, each having three degrees of freedom (x, y, z). It simulates hyperelastic, elastoplastic, and stress-hardened materials, capable of splitting under tension and crushing under compression. These elements are used to model concrete slabs with reinforcing bars, accurately representing nonlinear material behavior. Figure 3. shows the geometry.

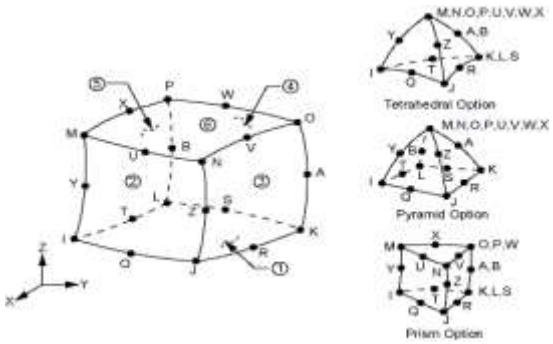

Fig. 3. Solid 186

2. CONTA174 (Contact Element)

CONTA174 is a 3D surface-to-surface contact element used to simulate the interaction between flexible and target surfaces in both normal and tangential directions. It is ideal for nonlinear contact, sticky behavior, and separation phenomena in 3D structure and coupled-field studies. CONTA174 was used to

model the interaction between the steel beam and concrete slab, ensuring realistic contact behavior. Figure 4. shows the geometry of the CONTA174 element.

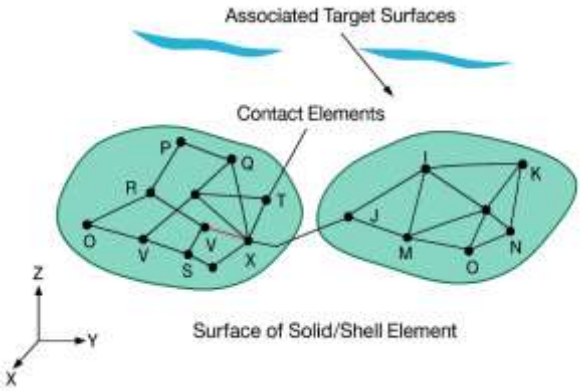

Fig. 4. CONTA 174

3. TARGET170 (Target Element)

The TARGET170 element represents the target surface in surface-to-surface contact analyses and works with the CONTA174 element to define contact pairs. It can be used with both rigid and deformable surfaces, specifying the geometric and physical properties of the contact interface. In the numerical model, TARGET170 elements were paired with CONTA174 to simulate the slab–beam interface, allowing for accurate pressure transfer, separation, and friction behavior. Figure 3.5 shows the geometry of the TARGET170 element.

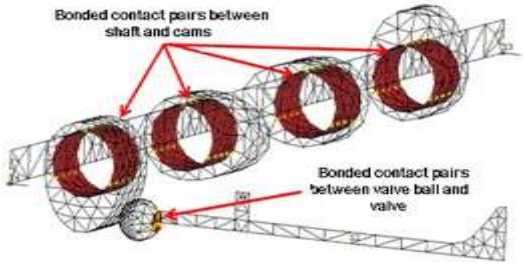

Fig. 5. TARGET 170

IV. CASE STUDY

Pre-Engineered Building (PEB) systems have emerged as a preferred solution for industrial, commercial, and storage facilities due to their speed of construction, cost efficiency, and structural adaptability. This case study examines the structural performance of castellated beams within a PEB shed located in Chakan, Pune, designed and developed by S. M. Kanitka, with architectural input from Mr. N. S. Dalvi. The structure adopts a single-span steel portal frame system in accordance with IS 800, incorporating moment connections, cold-formed roof sheeting, and built-up columns. The analysis encompasses the design of rafters, purlins, and columns under dead, live, and wind loads per IS 875, highlighting the site-specific conditions of a 12 m span, 30 m length, and 6 m eave height. By integrating castellated beams into the PEB framework, the study aims to assess enhancements in strength-to-weight ratio, structural efficiency, and serviceability while maintaining compliance with national design standards.

Fig 6. Third Eye view of actual site

SITE DETAILS

- Name of site: PEB structure
- Location of Site: Chakan, Pune
- A Proposed Shed is taken for case study location is in Chakan.
- Design Team: S. M. Kanitka
- Owner and Developer: S. M. Kanitka
- Architect: Mr. N S Dalvi
- Structural Engineer: S. M. Kanitka
- Builder: S. M. Kanitka

V. RESULTS AND DISCUSSION

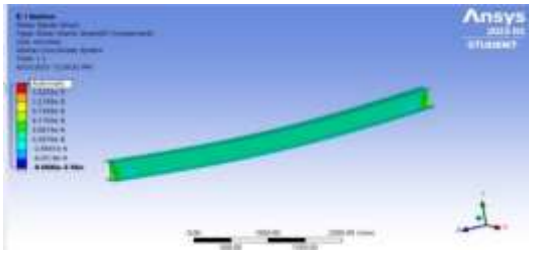

Fig 7. Shear Elastic Strain (XY Component) Distribution in an I-Section Beam – ANSYS Simulation

The shear elastic strain distribution in the I-section beam, as determined by an ANSYS simulation, ranges from -9.0696e-6 mm/mm to 1.5232e-5 mm/mm. The maximum strain occurs near the beam supports, while mild strain is observed at the mid-span. This indicates that the load is effectively transferred, and the structure is responding elastically to the applied load.

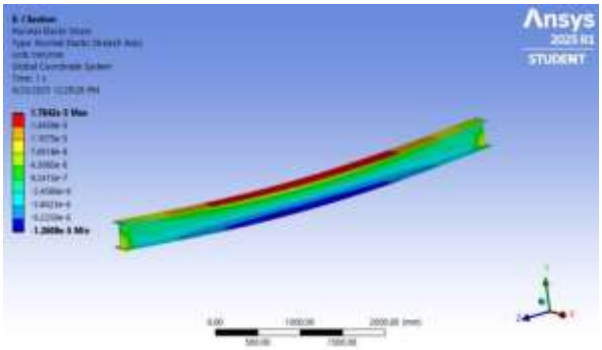

Fig 8. Normal Elastic Strain (X Axis) Distribution in an I-Section Beam – ANSYS Simulation

The normal elastic strain distribution along the X-axis of the I-section beam, analyzed using ANSYS, ranges from -1.2609e-5 mm/mm to 1.7842e-5 mm/mm. The top flange experiences the maximum tensile strain, while the bottom flange shows the most

compressive strain. This illustrates the bending behavior of the beam under applied load.

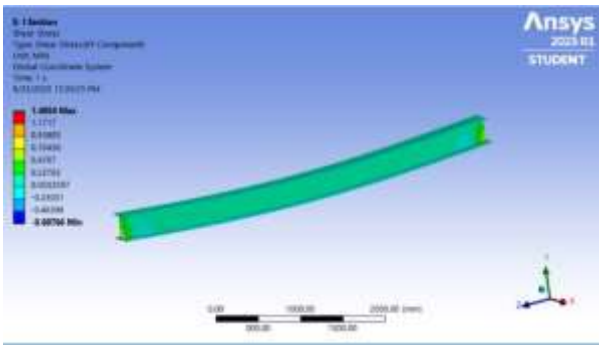

Fig 9. Shear Stress (XY Component) Distribution in an I-Section Beam ANSYS Simulation

The shear stress (XY component) distribution in the I-section beam, analyzed through ANSYS simulation, ranges from -0.69766 MPa to 1.4054 MPa. The highest shear stress occurs near the beam supports, while the lowest is observed at the mid-span. This indicates even load distribution and stable shear behavior when the load is applied to the beam.

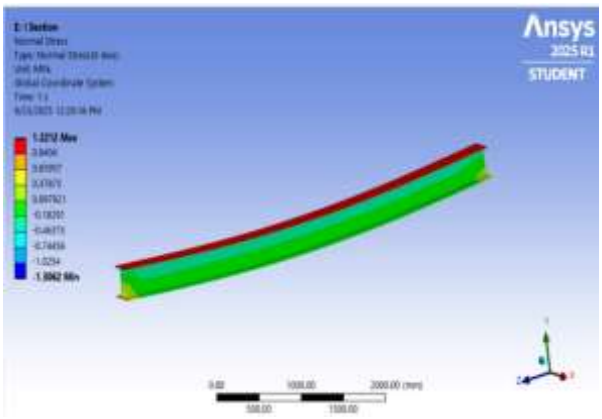

Fig 10. Normal Stress Distribution in I-Section Beam under Load

The normal stress (X-axis) distribution in the I-section beam, shown in Figure 5.4, reveals a tensile stress of 1.2212 MPa at the top flange and a compressive stress of -1.3062 MPa at the bottom flange. The stress transitions linearly across the section, indicating typical bending behavior, with the neutral axis located near the mid-depth region.

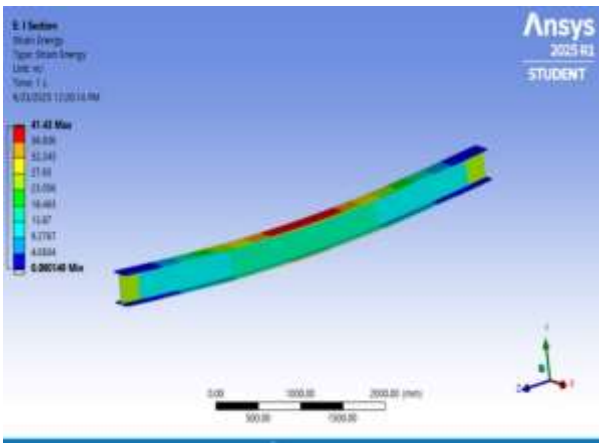

Fig 11. Strain Energy Distribution in I-Section Beam under Load

The strain energy distribution in the I-section beam subjected to loading shows a maximum strain energy of 41.43 mJ and a minimum of 0.0901 mJ. Higher strain energy is concentrated near the mid-span, indicating maximum deformation under bending. The energy gradually decreases towards the supports, reflecting minimal deformation at those regions.

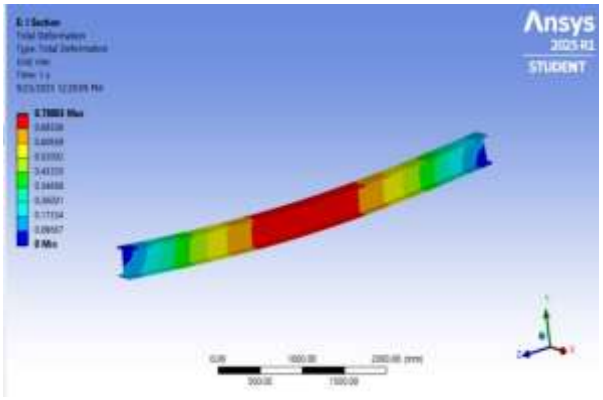

Fig 12. Total Deformation of I-Section Beam under Load

The I-section beam's deformation under external loading shows a maximum displacement of 0.78003 mm at the middle of the span (red area) and a minimum displacement of 0 mm near the supports (blue areas). The deformation pattern exhibits a smooth and symmetric deflection curve, indicating that the beam bends when the load is evenly distributed, with the greatest movement occurring at the mid-span.

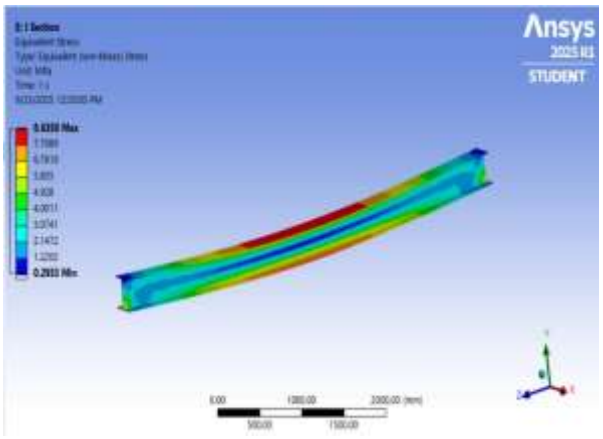

Fig 13. Equivalent (von-Mises) Stress Distribution in I-Section Beam

The von-Mises stress distribution in the I-section beam under load shows a maximum stress of 8.6358 MPa near the mid-span (red zone) and a minimum of 0.2933 MPa near the supports (blue zone). The stress pattern indicates that the bending stress is highest in the middle of the beam, as expected due to the load distribution.

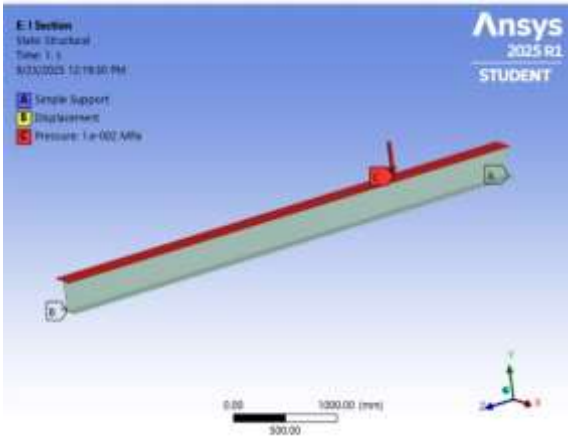

Fig 14. Boundary Conditions and Loading Setup for I-Section Beam

In the static structural analysis, the boundary conditions and pressure settings for the I-section beam are shown. At point A, the beam is supported simply, while point B has a movement limit to maintain stability during loading. A constant downward pressure of 1×10^{-2} MPa is applied at point C on the top lip, simulating an external force acting on the beam.

5.1 CASTELLATED SECTION

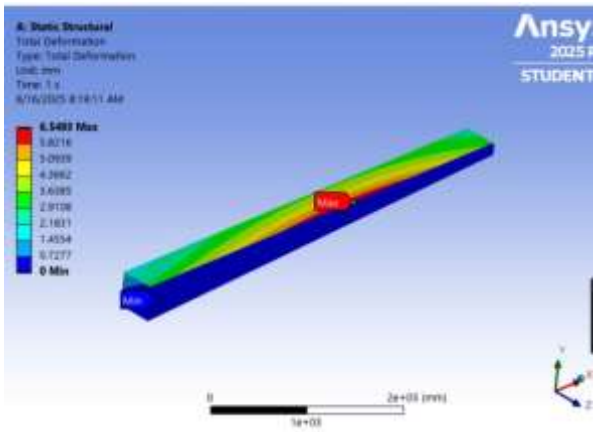

Fig 15. Total Deformation of Structural Model Under Static Load in ANSYS

The total displacement of the structure model under steady loading shows that the maximum deformation of 6.549 mm occurs near the middle of the span, while the minimum deformation of 0 mm is observed at the fixed support. The gradual color change from blue to red illustrates the variation in deformation along the beam's length, confirming normal bending behavior and efficient load distribution.

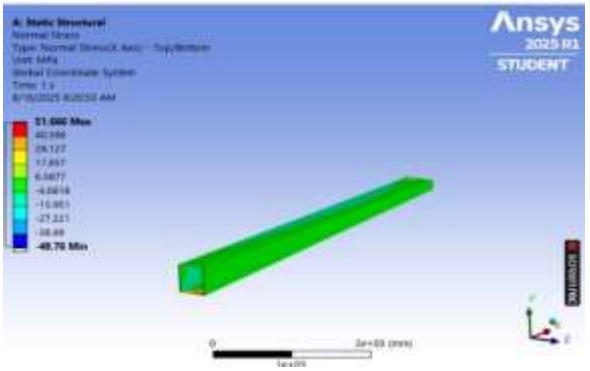

Fig 16. Normal Stress Distribution along the X-Axis.

The normal stress distribution along the X-axis of the structural model under static loading shows a maximum stress of 51.666 MPa at the top loaded region and a minimum compressive stress of -49.76 MPa at the bottom section. The stress pattern transitions from red (tension) to blue (compression), reflecting the bending behavior of the member and confirming the presence of both tensile and compressive stresses under the applied load.

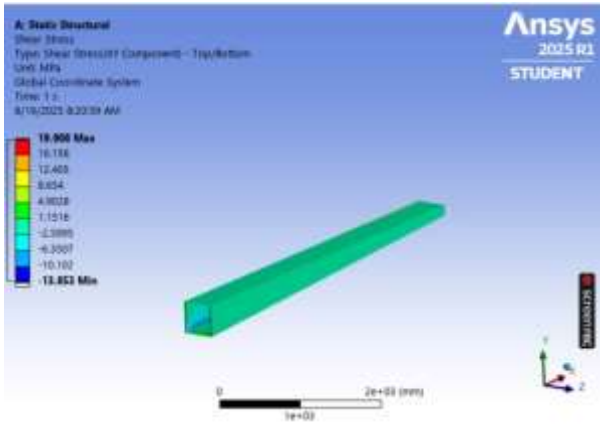

Fig 17. Shear Stress Distribution in Structural Beam

The shear stress distribution (XY component) in the structural beam under static loading shows a maximum shear stress of 19.908 MPa near the support region and a minimum shear stress of -13.853 MPa toward the opposite end. The color gradient from blue to red represents the variation in shear forces along the beam, confirming that maximum shear occurs near the supports, with lower shear toward the free end, in line with theoretical expectations.

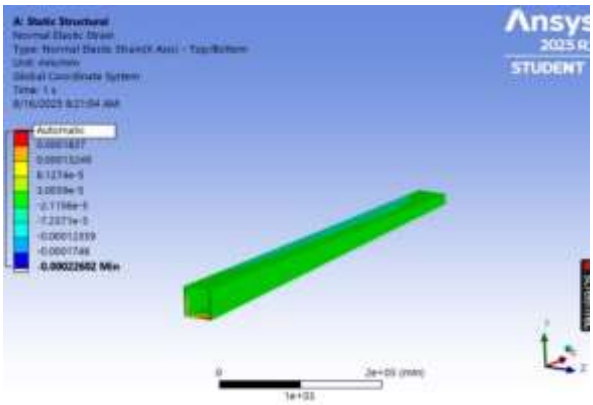

Fig 18. Normal Elastic Strain Distribution in Structural Member

The normal distribution of elastic strain along the X-axis shows a maximum strain of 0.0001837 mm/mm and a minimum strain of -0.00022602 mm/mm, both near the support region. The color change from blue to red indicates areas of compression and tension, confirming that the beam will bend normally under load.

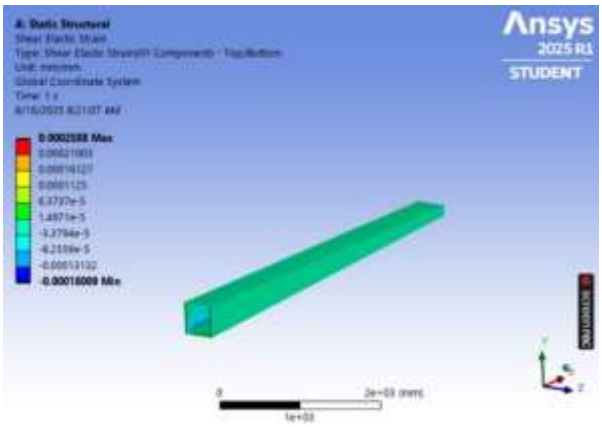

Fig 19. Shear Elastic Strain Distribution in a Structural Component

The shear elastic strain distribution in the structure, when not loaded, shows a range from 0.0002588 mm/mm at its highest point to -0.00018009 mm/mm at its lowest. The highest strain occurs near the support area, indicating deformation due to shear forces. The color shift from blue to red along the beam shows areas of least and most shear pressure.

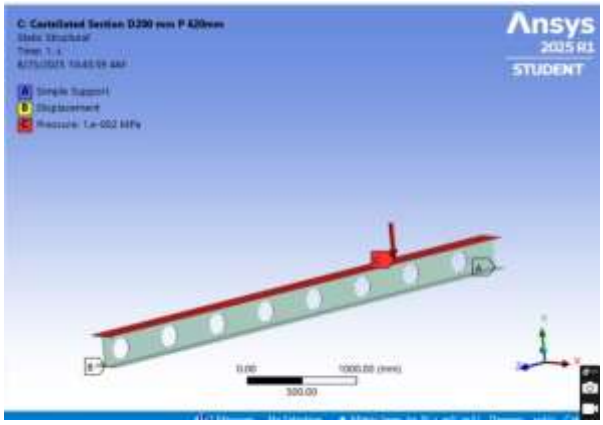

Fig 20. Castellated Section D200 mm P 620mm: Static Structural Analysis

The static structural analysis of a castellated beam section with a depth of 200 mm and a pitch of 620 mm shows that the beam is simply supported at point A and displaced at point B, with a uniform pressure of 1×10^{-2} MPa applied at point C on the top flange. The analysis illustrates the beam's deformation behavior and stress distribution under the applied load condition at time = 1 s.

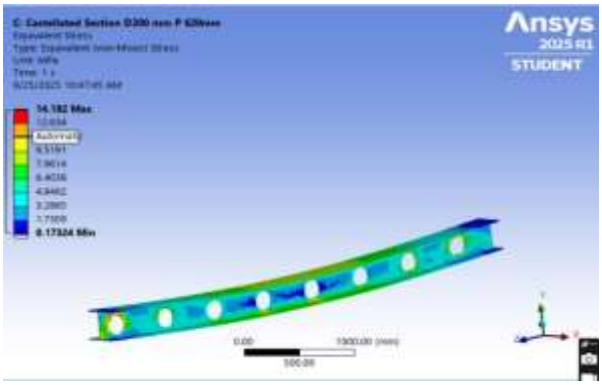

Fig 21. Stress Distribution in Castellated Section D200 mm P 620 mm

The equivalent (von-Mises) stress distribution in the castellated beam section with a depth of 200 mm and a pitch of 620 mm shows a maximum stress of 14.192 MPa near the web openings and support regions, while the minimum stress of 0.173 MPa is observed at the mid-span. The stress gradually decreases away from the load application point, indicating efficient load transfer through the castellated web.

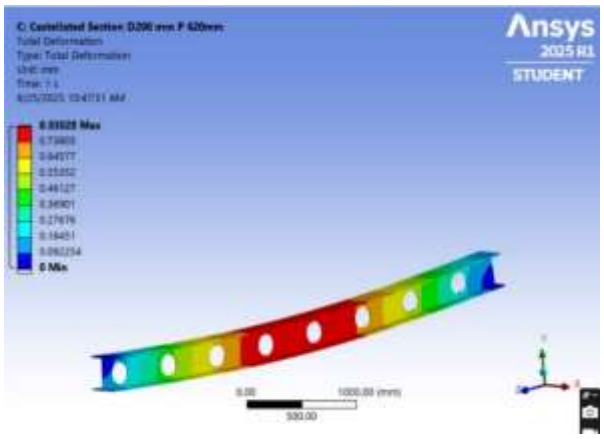

Fig 22 Total Deformation of Castellated Section D200 mm P 620mm

In the analysis, the castellated beam section with a depth of 200 mm and a pitch of 620 mm shows the overall deformation shape. The maximum deformation of 0.83028 mm occurs at the mid-span, while the least deformation (0 mm) is at the supports, where the pressure load is applied. The smooth bent curve of the deformation pattern confirms that the beam is structurally stable and efficiently distributes the load.

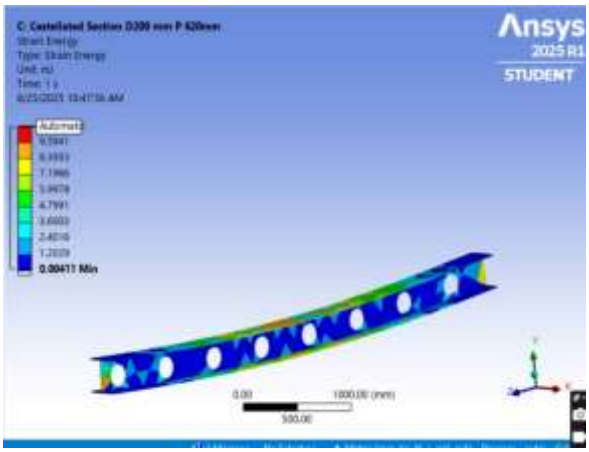

Fig 23 Strain Energy Distribution in Castellated Section D200 mm P 620mm

The strain energy distribution in the castellated beam section with a depth of 200 mm and a pitch of 620 mm shows a maximum strain energy of 9.5941 mJ near the web openings and load application region, with a minimum value of 0.00411 mJ at the supports. The energy absorption is concentrated around the cut-out zones, indicating areas of higher stress and deformation under the applied load.

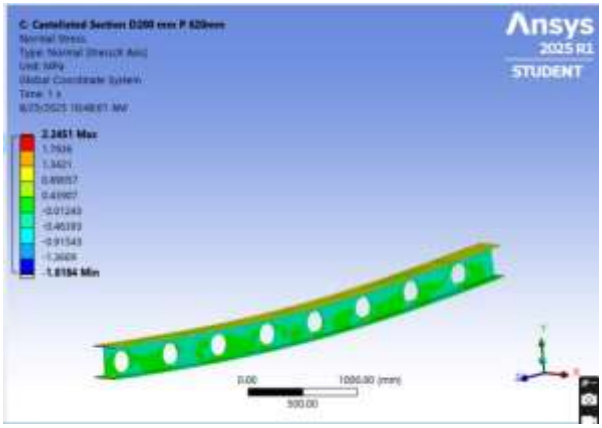

Fig 24 Normal Stress Distribution in Castellated Section D200 mm P 620mm

The normal stress distribution on the X-axis of the castellated beam section, with a depth of 200 mm and a pitch of 620 mm, shows the highest average stress of 2.2451 MPa and the lowest of -1.8184 MPa. Positive stress regions indicate tension along the top flange, while compressive stresses are observed near the bottom flange. The stress pattern confirms uniform bending behavior under the applied load, with stress concentration around the web openings.

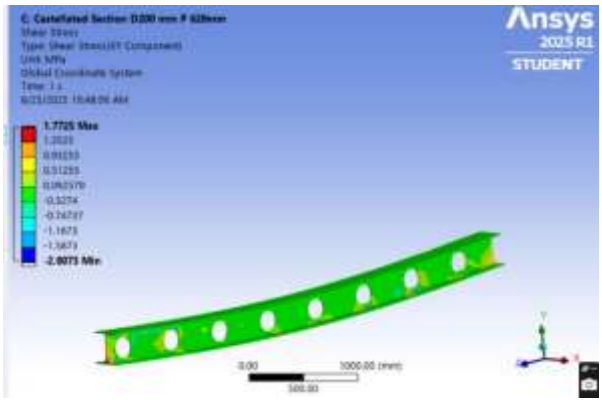

Fig 25 Shear Stress Distribution in Castellated Section D200 mm P 620 mm

The shear stress pattern for the castellated beam section (D200 mm, P620 mm) under load shows the highest shear stress of 1.7725 MPa and the lowest of -2.0073 MPa. The stress is concentrated around the web holes and supports, indicating significant shear activity in these areas. In the middle of the span, shear stress levels are more evenly distributed and lower.

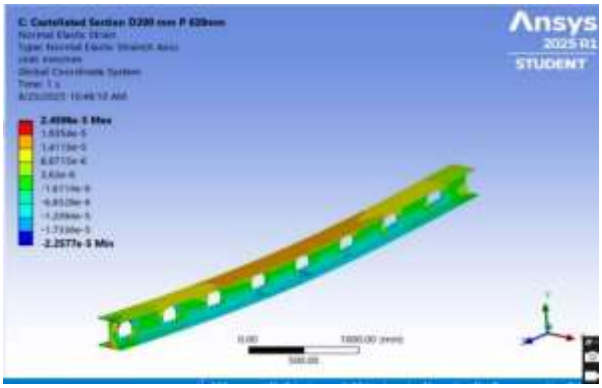

Fig 26 Normal Elastic Strain Distribution in Castellated Section D200 mm P 620mm

The normal elastic strain distribution along the castellated beam section (D200 mm, P620 mm) shows a maximum strain value of 2.4596×10^{-5} mm/mm and a minimum of -2.2577×10^{-5} mm/mm. Higher strain concentrations are observed near the top and bottom flanges, particularly around the web openings, indicating localized deformation under bending loads. The midspan region exhibits comparatively uniform strain behavior.

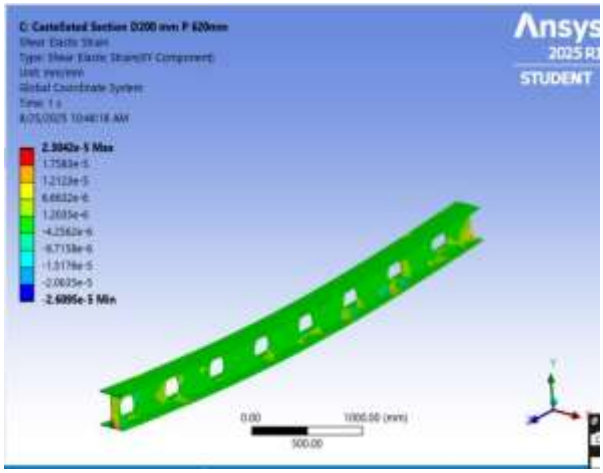

Fig 27 Shear Elastic Strain Distribution in Castellated Section

The shear elastic strain distribution for the castellated beam section (D200 mm, P620 mm) shows a maximum shear elastic strain of 2.3042×10^{-5} mm/mm and a minimum of -2.6095×10^{-5} mm/mm. Higher strain concentrations are observed around the circular openings and near the supports, indicating localized shear effects. The central region of the beam shows relatively uniform and lower strain values, demonstrating effective load transfer through the castellated geometry.

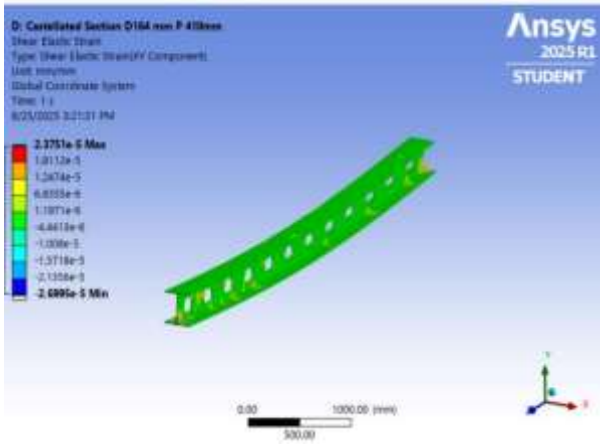

Fig 28 Shear Elastic Strain Distribution in Castellated Section

The shear elastic strain distribution for the castellated beam section (D164 mm, P410 mm) shows a maximum shear elastic strain of 2.3751×10^{-5} mm/mm and a minimum of -2.6995×10^{-5} mm/mm. Higher strain concentrations are observed near the web openings and support regions, indicating localized deformation under loading. The midspan area exhibits relatively uniform and lower strain, demonstrating stable shear behavior across the span.

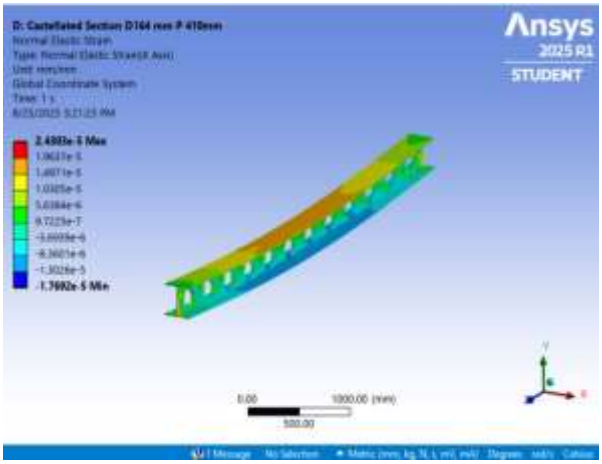

Fig 29 Normal Elastic Strain Distribution in Castellated Section

The normal elastic strain distribution for the castellated beam section (D164 mm, P410 mm) shows a maximum strain of 2.4303×10^{-5} mm/mm and a minimum strain of -1.7692×10^{-5} mm/mm. Higher strain values are observed along the top flange under compression and the bottom flange under tension, indicating bending behavior. The mid-web region shows moderate and uniform strain, signifying effective structural performance under loading.

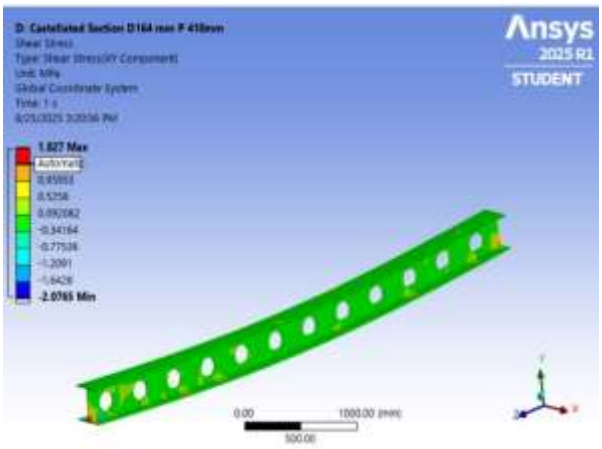

Fig 30. Shear Stress Distribution in Castellated Section D164 mm P 410mm

In the castellated beam section (D164 mm, P410 mm), the shear stress distribution shows a maximum shear stress of 1.827 MPa and a minimum of -2.0765 MPa. Stress concentration is primarily observed around the openings and near the supports, while the mid-span region experiences relatively lower stress values, indicating a uniform stress distribution along the web.

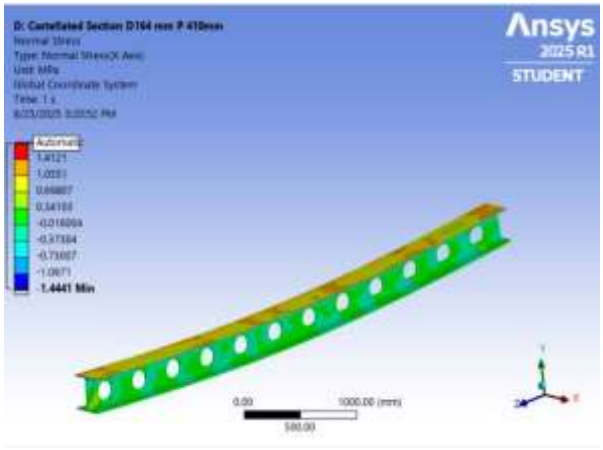

Fig 31. Normal Stress Distribution in Castellated Section (D164 mm P 410 mm) under Applied Load

When a load is applied to the castellated beam section (D164 mm, P410 mm), the normal stress distribution shows a maximum stress of 1.4121 MPa and a minimum of -1.4441 MPa. Higher stress concentrations occur near the top and bottom edges, especially around the web holes, indicating tensile and compressive stresses. The mid-web region, however, experiences lower stress strength.

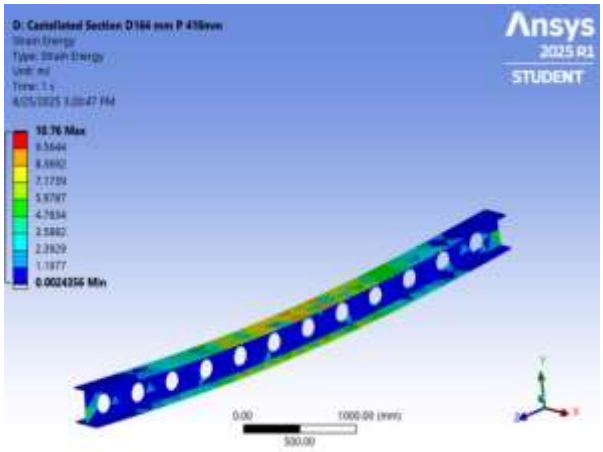

Fig 32. Strain Energy Distribution in Castellated Section D164 mm P 410mm

The strain energy distribution in the castellated beam section (D164 mm, P410 mm) shows a maximum of 10.76 mJ and a minimum of 0.0024356 mJ. Higher energy concentrates near web openings and supports, indicating zones of greater deformation and stress transfer, while the remainder exhibits lower energy, reflecting relatively uniform load distribution.

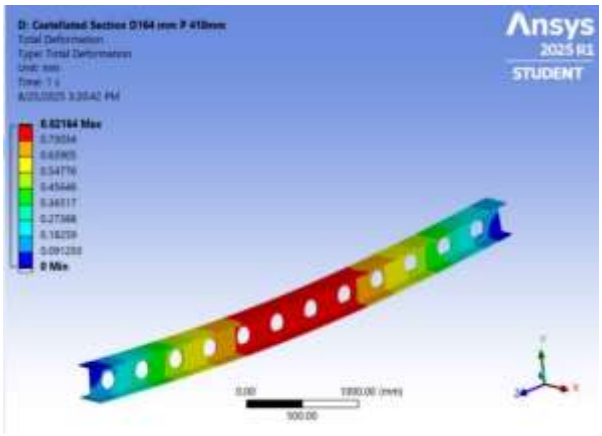

Fig 33. Total Deformation of Castellated Section D164 mm P 410mm

The total deformation of the castellated beam section (D164 mm, P410 mm) shows a maximum change of 0.82164 mm and a minimum of 0 mm. The beam deforms most in the middle of the span and less near the supports. This indicates that the beam behaves as expected under load, with the majority of the movement occurring in the middle due to bending.

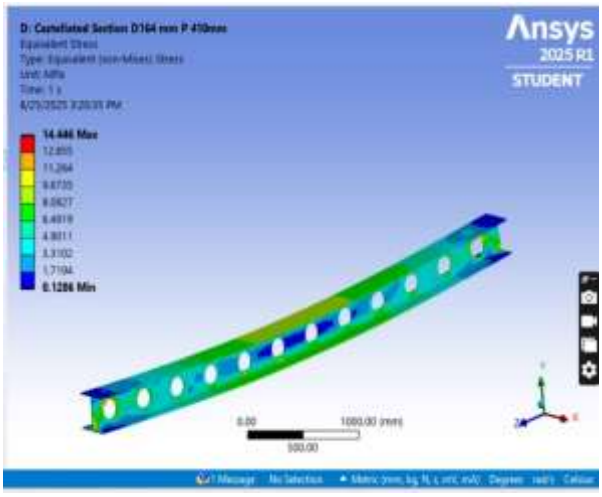

Fig 34. Equivalent Stress Distribution in Castellated Section

The equivalent (von-Mises) stress distribution in the castellated beam section (D164 mm, P410 mm) shows a maximum stress of 14.446 MPa and a minimum of 0.1286 MPa. Higher stress concentrations are observed around the web openings and near the supports, indicating potential critical failure points. The rest of the beam experiences relatively lower stress, suggesting efficient load transfer through the section.

Table 2. Total Deformation (mm) for Different Beam Sections

Total Deformation (Mm)			
I Section	Tube Section 1	Castellated Beam 2	Castellated Beam3
1.3	0.83	0.8	0.79

The comparison of total deformation (in mm) across different beam sections under applied loads shows that the tapered section exhibits the highest deformation at 2.6 mm, indicating greater flexibility. Among the castellated beams, Beam 1 shows the highest deformation at 0.83 mm, while Beam 2 and Beam 3 demonstrate slightly lower deformations at 0.8 mm and 0.79 mm, respectively. This suggests that the castellated beams provide better structural stiffness and resistance to deformation.

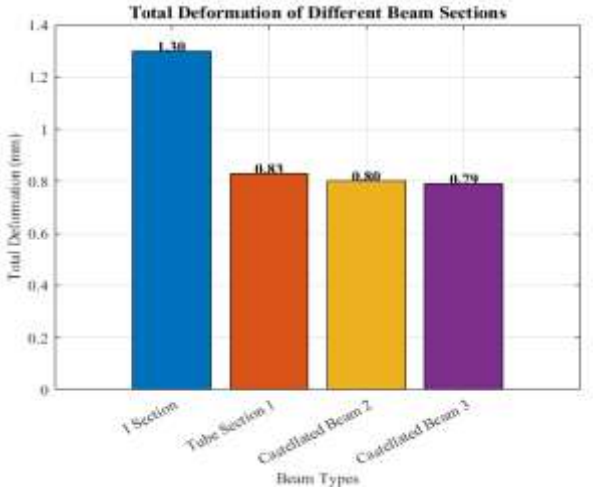

Fig 35. Total deformation

The total deformation comparison of various beam types shows that the Tapered I Section experiences the most deformation at 1.3 mm. In contrast, the castellated beams exhibit significantly lower deformations, with Beam 1 at 0.83 mm, Beam 2 at 0.8 mm, and Beam 3 at 0.79 mm. This indicates that castellated beams are more resistant to deformation compared to the Tapered I Section.

Table 3. Normal Stress (MPa) for Different Beam Sections

Normal Stress (mm)			
I Section	Tube Section 1	Castellated Beam 2	Castellated Beam3
2.39	1.79	1.41	1.42

The normal stress values (in MPa) for various beam sections show that the tapered section experiences a significantly higher stress of 40.39 MPa, indicating greater resistance to the applied load. In comparison, the castellated beams exhibit much lower normal stress, with Beam 1 at 1.79 MPa, Beam 2 at 1.41 MPa, and Beam 3 at 1.42 MPa. These results demonstrate that the castellated beams experience considerably less stress, highlighting their improved structural efficiency and better load distribution compared to the tapered section.

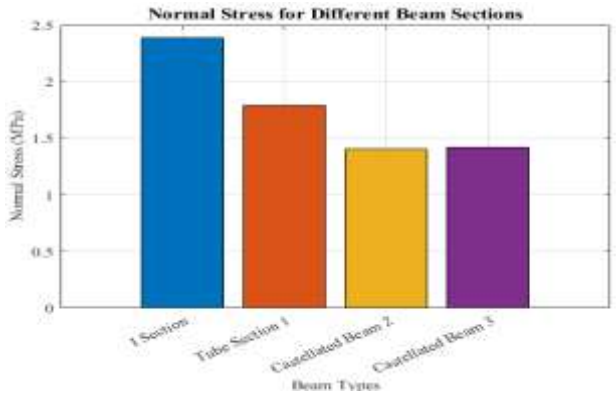

Fig 36. Normal stress

The comparison of normal stress across different beam types shows that the Tapered I Section experiences the highest normal stress at 2.5 mm, followed by Castellated Beam 1 at 1.8 mm. Castellated Beams 2 and 3 exhibit slightly lower stresses around 1.6 mm. This indicates that the Tapered I Section is subject to the highest stress compared to the castellated beams.

Table 4. Shear Stress (MPa) for Different Beam Sections

Shear Stress			
I Section	Tube Section 1	Castellated Beam 2	Castellated Beam3
2.85	1.35	1.82	1.92

The shear stress comparison for various beam sections shows that the tapered section experiences the highest shear stress at 16.15 MPa, indicating a higher tendency to resist shear forces. In contrast, the castellated beam sections exhibit significantly lower shear stress values, with Beam 1 at 1.35 MPa, Beam 2 at 1.82 MPa, and Beam 3 at 1.92 MPa. These findings suggest that the castellated beams provide better shear resistance and more efficient load transfer compared to the tapered section.

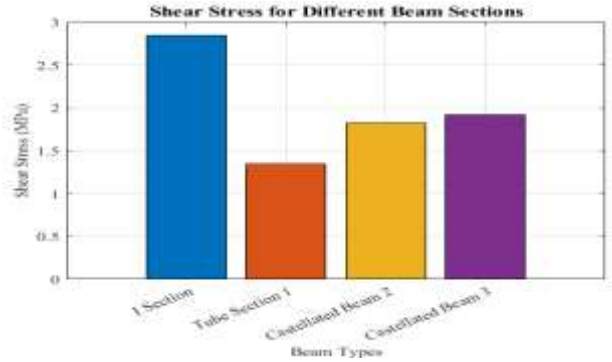

Fig 37. Shear stress

The shear stress comparison between different beam types shows that the Tapered I Section experiences the highest shear stress at approximately 3.2 mm, significantly higher than the Castellated Beams, which range from 1.7 mm to 2.0 mm. This indicates that the Tapered I Section experiences much more shear stress compared to the castellated beams.

Table 5. Base Shear (kN) for Different Beam Sections

Base Shear			
I Section	Tube Section 1	Castellated Beam 2	Castellated Beam3
1.62	1.60	1.59	1.57

The comparison of base shear values shows that the I Section exhibits the highest base shear of 1.62 kN, indicating greater resistance to lateral loads. The Tube Section follows with 1.60 kN, and the Castellated Beams show slightly lower values at 1.59 kN and 1.57 kN, suggesting marginally reduced stiffness. Overall, all beam types demonstrate comparable stability under seismic or lateral loading conditions.

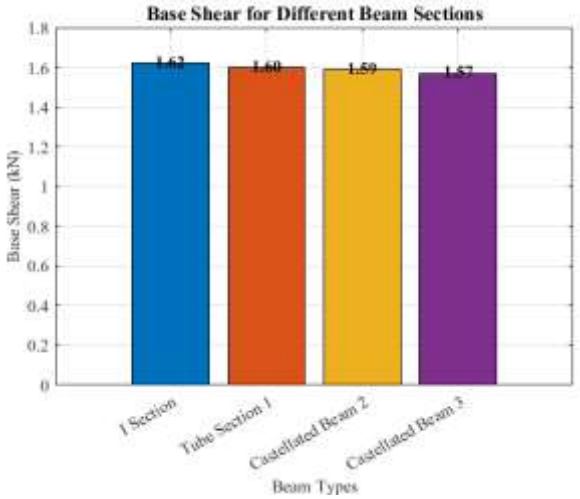

Fig 38. Base Shear Comparison for Different Beam Sections

The I Section has the highest base shear value of 1.62 kN, indicating superior resistance to lateral loads. The Tube Section (1.60 kN) and Castellated Beams (1.59 kN and 1.57 kN) show slightly lower values, suggesting minor reductions in stiffness. Overall, all sections exhibit similar performance, reflecting stable structural behavior under seismic or wind-induced forces.

Table 6. Story Drift (mm) for Different Beam Sections

Story Drift			
I Section	Tube Section 1	Castellated Beam 2	Castellated Beam3
7.2	6.8	6.5	6.3

The I Section has the highest story drift value of 7.2 mm, indicating greater lateral movement under load. The Tube Section shows a slightly lower drift of 6.8 mm, while the Castellated Beams have even lower values at 6.5 mm and 6.3 mm. This reduction in drift suggests that castellated beams offer improved stiffness and resistance to deformation, enhancing structural stability under lateral forces.

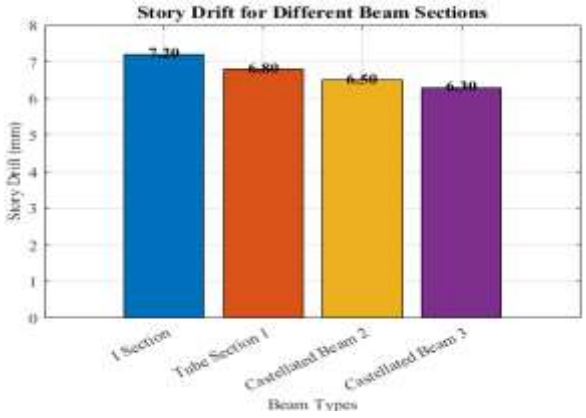

Fig 39. Story Drift Comparison for Different Beam Sections

The I Section exhibits the highest story drift value of 7.2 mm, indicating greater lateral displacement under applied loads. The Tube Section shows a slightly lower drift of 6.8 mm, while the Castellated Beams show further reductions at 6.5 mm and 6.3

mm. This decrease in story drift demonstrates that castellated beams offer better stiffness and structural control, enhancing lateral stability and minimizing deformation compared to traditional beam sections.

Table 7 Bending Moment (kN·m) for Different Beam Sections

Bending Moment			
I Section	Tube Section 1	Castellated Beam 2	Castellated Beam3
100.0	98.0	105.0	106.0

The comparison of bending moment values shows that Castellated Beam 3 has the highest bending moment of 106.0 kN·m, followed closely by Castellated Beam 2 with 105.0 kN·m. The I Section and Tube Section exhibit lower values of 100.0 kN·m and 98.0 kN·m, respectively. This indicates that castellated beams can sustain higher bending moments due to their enhanced depth and structural efficiency. Overall, castellated beams demonstrate superior bending strength compared to conventional sections.

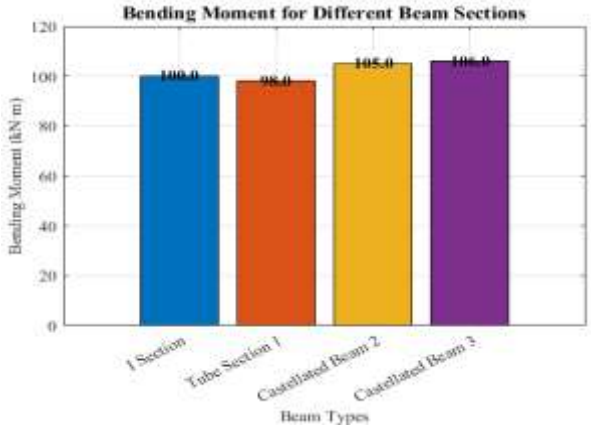

Fig 40. Bending Moment Comparison for Different Beam Sections

Castellated Beam 3 shows the highest bending moment value of 106.0 kN·m, followed closely by Castellated Beam 2 at 105.0 kN·m. The I Section and Tube Section have lower values of 100.0 kN·m and 98.0 kN·m, respectively. This indicates that castellated beams have a greater moment-carrying capacity due to their enhanced depth and improved section modulus. Overall, castellated beams exhibit superior bending performance and higher structural efficiency compared to conventional beam types.

Table 8 Axial Force (kN) for Different Beam Sections

Axial Force (kN)			
I Section	Tube Section 1	Castellated Beam 2	Castellated Beam3
200.0	198.0	203.0	204.0

Castellated Beam 3 experiences the highest force of 204.0 kN, followed closely by Castellated Beam 2 at 203.0 kN. The I Section and Tube Section carry slightly lower axial loads of 200.0 kN and 198.0 kN, respectively. This indicates that castellated beams have superior load-carrying capacity and structural efficiency under axial compression. Overall, castellated configurations offer enhanced strength and stability compared to conventional beam sections.

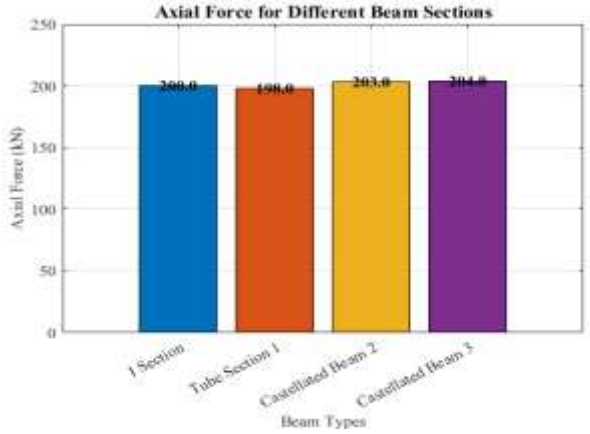

Fig 41 Axial Force Comparison for Different Beam Sections

Castellated Beam 3 records the highest axial force of 204.0 kN, followed closely by Castellated Beam 2 at 203.0 kN. The I Section and Tube Section exhibit slightly lower values of 200.0 kN and 198.0 kN, respectively. This suggests that castellated beams have superior load-carrying capacity and can withstand higher axial compression forces. Overall, castellated beams demonstrate better strength and stability compared to traditional beam sections.

Table 9 Torsion (kN·m) for Different Beam Sections

Torsion			
I Section	Tube Section 1	Castellated Beam 2	Castellated Beam3
8.0	7.6	9.2	9.5

Castellated Beam 3 exhibits the highest torsional value of 9.5 kN·m, followed by Castellated Beam 2 at 9.2 kN·m. The I Section and Tube Section record lower values of 8.0 kN·m and 7.6 kN·m, respectively. This indicates that castellated beams offer superior torsional resistance due to their enhanced geometry and stiffness. Overall, castellated beams perform better in resisting twisting effects under applied loads.

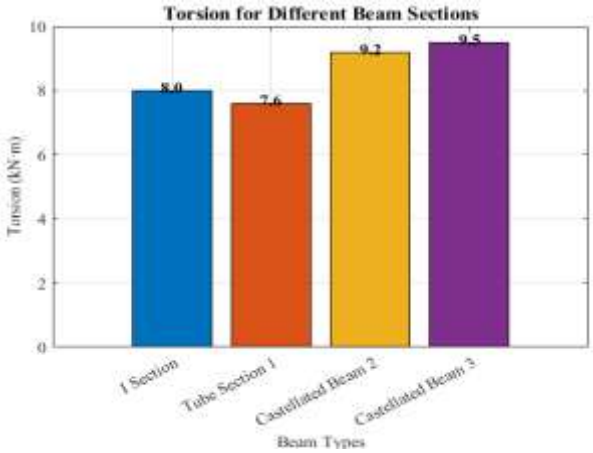

Fig 42 Torsion Comparison for Different Beam Sections

Castellated Beam 3 shows the highest torsional resistance of 9.5 kN·m, followed by Castellated Beam 2 at 9.2 kN·m. The I Section and Tube Section 1 exhibit lower torsional strengths of 8.0 kN·m and 7.6 kN·m, respectively. This indicates that castellated beams, due to their enhanced geometry and material

distribution, offer superior torsional performance compared to conventional beam sections.

Table 10 Shear Force (kN) for Different Beam Sections

Shear Force			
I Section	Tube Section 1	Castellated Beam 2	Castellated Beam3
75.0	68.0	78	80.0

The Tube Section 1 recorded the lowest shear force of 68.0 kN, while Castellated Beam 3 exhibited the highest value of 80.0 kN. The I-Section and Castellated Beam 2 showed intermediate values of 75.0 kN and 78.0 kN, respectively. These results indicate that castellated beam configurations enhance shear strength compared to tubular and conventional I-sections due to increased web area and stiffness.

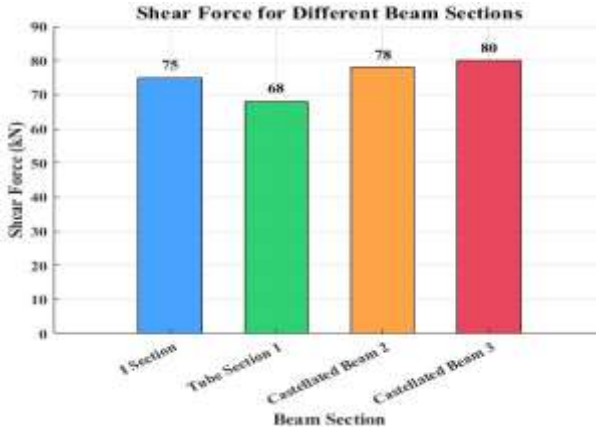

Fig 43 Shear Force Comparison for Different Beam Sections

The variation in shear force values shows 68.0 kN for Tube Section 1, 75.0 kN for I-Section, 78.0 kN for Castellated Beam 2, and 80.0 kN for Castellated Beam 3. The rising trend indicates that castellated beams outperform the other sections, confirming that Castellated Beam 3 achieves the highest shear resistance among all tested beam types.

VI. CONCLUSION

This study investigated the structural performance of castellated beams incorporated into Pre-Engineered Buildings (PEBs) and compared them with conventional solid web beams using finite element analysis (FEA). Castellated beams, produced by introducing hexagonal or circular openings in rolled I-sections, provide significant advantages such as a higher strength-to-weight ratio, increased load-carrying capacity, and material savings. Their enhanced moment of inertia improves bending resistance without increasing weight, making them especially suitable for long-span applications. The results revealed that castellated beams experience slightly higher deflections than solid web beams, particularly under gravity loading conditions, due to reduced stiffness from web openings. However, these deflections remain within permissible serviceability limits. In terms of bending strength and load distribution, castellated beams outperformed solid beams, thus offering an efficient and economical alternative. A key observation was the presence of stress concentrations around the web openings, especially in shear-dominant regions, which pose a risk of local failure if not carefully designed.

In conclusion, castellated beams present an efficient and cost-effective option for PEB structures, combining superior load performance with material optimization. With appropriate reinforcements and improved detailing, they can overcome issues of stress concentration and deflection, making them highly suitable for future applications, including seismic and dynamic load scenarios.

VI. FUTURE SCOPE

The future scope of research on castellated beams in Pre-Engineered Buildings (PEBs) offers multiple directions for advancement in design, materials, and applications. One promising area is the integration of advanced materials such as high-strength steel alloys, composites, and hybrid materials. These innovations could enhance load-carrying capacity, reduce self-weight, and mitigate serviceability concerns like deflection. Additionally, the seismic and dynamic performance of castellated beams requires further exploration, particularly for their application in earthquake-prone regions. Studies focused on energy dissipation, ductility, and resilience under cyclic loading can significantly strengthen their reliability. Another key area is the optimization of web opening geometries. Beyond conventional hexagonal and circular patterns, parametric studies on varied hole shapes, sizes, and spacing could minimize stress concentrations while maximizing efficiency. Sustainability analysis is equally vital; life-cycle assessments comparing castellated and solid beams would provide valuable data for reducing embodied carbon in construction. The integration of computational intelligence through AI and machine learning tools could automate optimization processes and guide innovative designs.

Finally, experimental validation remains essential. Large-scale testing of castellated beams under real loading scenarios would bridge the gap between finite element predictions and practical performance, leading to refined design codes and broader industry adoption.

VII. REFERENCES

1. C. V. Reddy and K. Subhashini, “Lightweight Composite Ferrocement Structural Elements: A Review,” 2018.
2. M. F. Ghazy, M. A. Abd Elaty, M. Taman, and M. E. Eissa, “Durability performance of geopolymer ferrocement panels prepared by different alkaline activators,” *Structures*, vol. 38, pp. 168–183, Apr. 2022, doi: 10.1016/j.istruc.2022.01.087.
3. G. Murali *et al.*, “Structural Behavior of Fibrous-Ferrocement Panel Subjected to Flexural and Impact Loads,” *Materials*, vol. 13, no. 24, p. 5648, Dec. 2020, doi: 10.3390/ma13245648.
4. D. Gopal and D. Shobarajkumar, “Comparative study on structural behavior of ferrocement wall panels,” *Earthq. Eng. Struct. Dyn.*, vol. 53, no. 5, pp. 1727–1741, Apr. 2024, doi: 10.1002/eqe.4081.
5. Z. Liu, P. Van Den Heede, and N. De Belie, “Effect of the Mechanical Load on the Carbonation of Concrete: A Review of the Underlying Mechanisms, Test Methods, and Results,” *Materials*, vol. 14, no. 16, p. 4407, Aug. 2021, doi: 10.3390/ma14164407.
6. N. D. Yılmaz and G. M. Arifuzzaman Khan, “Flexural behavior of textile-reinforced polymer composites,” in *Mechanical and Physical Testing of Biocomposites, Fibre-Reinforced Composites and Hybrid Composites*, Elsevier,

2019, pp. 13–42. doi: 10.1016/B978-0-08-102292-4.00002-3.
7. L. K. Idriss and M. Owais, "Global sensitivity analysis for seismic performance of shear wall with high-strength steel bars and recycled aggregate concrete," *Constr. Build. Mater.*, vol. 411, p. 134498, Jan. 2024, doi: 10.1016/j.conbuildmat.2023.134498.
8. Q. D. Nguyen and A. Castel, "Long-term durability of underground reinforced concrete pipes in natural chloride and carbonation environments," *Constr. Build. Mater.*, vol. 394, p. 132230, Aug. 2023, doi: 10.1016/j.conbuildmat.2023.132230.
9. P. Sharma, "Analytical Research on Ferrocement : Design, Strength and Servicibility Aspects," 2016.
10. Y. Zhang, H. Li, Y. Gamil, B. Iftikhar, and H. Murtaza, "Towards modern sustainable construction materials: a bibliographic analysis of engineered geopolymer composites," *Front. Mater.*, vol. 10, p. 1277567, Oct. 2023, doi: 10.3389/fmats.2023.1277567.